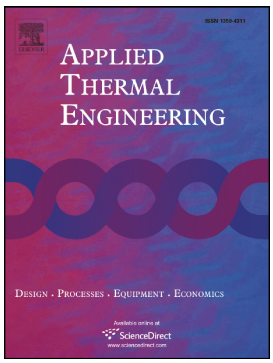

Environmental and thermophysical pre-selection of low-melting point molten salts for thermal energy storage in concentrated solar power systems

M. Botejara-Antúnez, J. Chaves, M.I. Lasanta, G. García-Martín, A. Rivero-Cacho, J. García-Sanz-Calcedo, F.J. Pérez

PII: S1359-4311(26)02002-8

DOI: https://doi.org/10.1016/j.applthermaleng.2026.131694

Reference: ATE 131694

To appear in:

Received date: 27 March 2026

Revised date: 18 May 2026

Accepted date: 29 May 2026

Please cite this article as: M. Botejara-Antúnez, J. Chaves, M.I. Lasanta, et al., Environmental and thermophysical pre-selection of low-melting point molten salts for thermal energy storage in concentrated solar power systems, (2024), https://doi.org/10.1016/j.applthermaleng.2026.131694

Environmental and thermophysical pre-selection of low-melting point molten salts for thermal energy storage in concentrated solar power systems

Botejara-Antúnez M.[1], Chaves J.[2*], Lasanta M. I.[2], García-Martín G.[2], Rivero-Cacho A.[1], García-Sanz-Calcedo J.[1] and Pérez F. J.[2]

[1]Department of Graphical Expression, School of Industrial Engineering, University of Extremadura, Elvas Avenue s/n, Badajoz, Spain.

[2]Chemical and Materials Engineering Department, Complutense University of Madrid, Pl. Ciencias 2, Madrid, Spain.

[*]Corresponding author: jachaves@ucm.es (J. Chaves)

Abstract:

Environmental impact, energy efficiency, and cost optimization are key factors during the strategic selection of Thermal Energy Storage materials for concentrated solar power plants, where low-melting point Molten Salts are positioned as one of the preferred alternatives due to their operational stability, high heat capacity, and low vapor pressure. In this study, 12 low-melting point Molten Salts were thermophysically characterized (the traditional Solar Salt, Hitec®, Hitec XL®, and 9 new formulations), and their environmental performance per unit of heat transfer was assessed using SimaPro 10.1 software, the ReCiPe 2016 assessment method, the Ecoinvent 3.11 database, and the "cradle-to-grave" approach. The results show that the $LiNO_3$ Molten Salts, specifically Salt #5, have the best thermophysical properties and the lowest impact values (95.29 mPt/MJ), and achieved the more favorable results in 7 of 22 impact categories and in the three damage areas for intermediate cost values per unit of heat transfer (2.88 €/MJ). Furthermore, it is found that Solar Salt obtained the highest environmental impact score (335.44 mPt/MJ). The novelty of this work lies in the combined thermophysical and environmental pre-selection of low-melting point Molten Salts per unit of heat transfer. The knowledge gained in this study will provide a detailed view of the environmental impacts of concentrated solar power plants, thereby improving decision-making criteria for responsible managers and contributing to the decarbonization of the energy sector.

Keywords: CSP, TES, Low-melting point Molten Salts, Life Cycle Assessment, Environmental Impacts.

1. Introduction

Concentrated solar power (CSP) has emerged as a leading renewable energy technology due to its unique ability to integrate cost-effective thermal energy storage (TES), enabling dispatchable electricity generation [1,2]. Unlike photovoltaic systems, CSP plants can

store excess thermal energy during peak sunlight hours and release it when needed, addressing the critical challenge of intermittency in renewable energy [3]. At the heart of this capability are molten salts, which serve as both heat transfer fluids (HTFs) and thermal storage media in modern CSP systems [4,5].

Current CSP technologies primarily employ two types of solar concentrators: line-focus systems, such as parabolic troughs (operating below 550°C), and point-focus systems, like central towers (capable of exceeding 700°C) [6,7]. While parabolic trough plants represent the most mature technology, their reliance on synthetic oils as HTFs creates significant limitations [8]. These oils degrade above 390°C and require complex indirect storage systems with heat exchangers [9]. Moreover, life cycle assessments reveal that synthetic oils have substantially higher environmental impacts compared to molten salt alternatives [10].

Nitrate-based molten salts have become the preferred TES medium due to their favorable thermophysical properties, including high heat capacity (1.4 - 1.6 kJ/kg·K), low vapor pressure, and operational stability up to 600°C [11,12]. Three commercial formulations currently dominate CSP applications: Solar Salt (60%$NaNO_3$ - 40%KNO_3), Hitec® (53%KNO_3 - 40%$NaNO_2$ - 7%$NaNO_3$), and Hitec XL® (48%$Ca(NO_3)_2$ - 7%$NaNO_3$ - 45%KNO_3) [13,14]. While these salts offer significant advantages over synthetic oils, each presents unique challenges that limit their performance. Solar Salt's relatively high melting point (227°C) creates freezing risks in piping systems [15,16], Hitec®'s nitrite content oxidizes above 350°C [17], and Hitec XL®'s calcium nitrate component introduces hygroscopicity issues that complicate handling and storage [18,19].

The CSP industry urgently needs improved salt formulations that combine lower melting points (<150°C), higher thermal stability (>600°C), and reduced corrosivity while maintaining cost-effectiveness [20]. Recent research has focused on developing advanced ternary and quaternary nitrate mixtures incorporating lithium, calcium, sodium, and potassium cations to optimize these properties [21]. Particular attention has been given to calcium-containing salts due to their ability to lower melting points significantly, though their hygroscopic nature and potential for oxide formation require careful consideration [22]. Additionally, lithium-containing salt has been studied as this does increase the thermal stability while lowering the melting point of the salt [23]. However, the price of lithium tends to increase the costs of formulation [24].

Several novel studies are investigating different ternary and quaternary compositions to identify the most cost-effective composition while enhancing the salts' thermophysical properties [25,26]. Other recent studies have reported that adding nanoparticles enhances the thermophysical properties of molten salts, including Solar Salt and HITEC [27]. In this regard, authors such as Gurgenc et al. (2025, 2026) investigated methods to improve the thermophysical properties of Solar Salt by adding various nanoparticles. In an initial study, they assessed the potential to enhance heat capacity and thermal conductivity by adding B_4C [28], whereas in a second study, they evaluated the potential to enhance density and thermal stability by adding HfB_2, TiB_2, and ZrB_2 nanoparticles [29]. Lastly, in parallel, they transferred both studies to Molten Salt HITEC®, evaluating its potential for improvement by adding TiB_2, ZrB_2 nanoparticles [30].

In this context and given the need to advance in the decarbonization of the energy sector [31], it is essential to incorporate new materials and develop studies that analyze not only technical and economic criteria, but also sustainable aspects [32]. However, the environmental dimension of CSP technology remains largely underexplored, with only a limited number of studies available. Furthermore, few papers have applied Life Cycle Assessment (LCA) to quantify its environmental performance [33–35].

Scientific production in this area has focused mainly on the Life Cycle Assessment (LCA) of the CSP plants [36]. Along these lines, Piemonte et al. (2011) compared their environmental impacts with those of conventional oil and gas plants [37]. Subsequent studies, such as those by Ehtiwesh et al. (2016) or Ko et al. (2018), assessed the environmental impact and the life cycle cost of plants with Molten Salt technology [38,39]. Other authors, such as Li et al. (2019), defined new LCA models to characterize the carbon footprint of CSP plants with parabolic trough technology [40]. Gasa et al. (2021, 2022) compared different solar tower CSP plants differentiated by the presence or absence of thermal storage technologies [41,42]. Xiao et al. (2022) assessed the environmental performance of CSP plants integrated with air-cooled supercritical Brayton cycles [43]. Finally, Qi et al. (2024, 2025) analyzed the environmental benefits and economic performance associated with hybridizing CSP technology with photovoltaic solar technology [44,45].

Regarding TES technology, Adeoye et al. (2014) compared two systems, one for storing sensible heat in high-temperature concrete and another for storing it using Molten Salts [46]. Miró et al. (2015) introduced a thermal storage system based on Phase-Change Materials (PCMs) [47]. Along these lines, Lalau et al. (2016) quantified the environmental footprint of an alternative TES technology based on recycled industrial ceramics [48]. Thaker et al. (2019) conducted LCA studies to assess the benefits of thermal storage systems in the reduction of the environmental impacts associated with CSP plants [49]. Finally, Le Roux et al. (2024) explored the optimal geometry in the sustainable design of Molten Salt TES systems for CSP plants operating with HTF thermal oil [50].

Numerous authors have also assessed the introduction of new TES materials to reduce the environmental impact associated with their life cycle [51]. Ramón-Álvarez et al. (2023) proposed the inclusion of alkalized materials, which demonstrated significant reductions in the water and energy footprint [52]. Vielma Leal et al. (2023) introduced TES materials based on steel slag from electric arc furnaces (EAFs) [53]. Finally, Betancor-Cazorla et al. (2025) assessed the environmental performance of new blended tertiary cements (LC3) [54].

Regarding heat transfer fluids, current scientific publications focus on the design, characterization, and techno-economic assessment of new proposals to guarantee the technical operating requirements while minimizing the plant execution and operating costs [55]. However, few publications have considered environmental dimensions. Among these, the study by Batuecas et al. (2017) stands out that it assessed the environmental performance of the Therminol VP-1®, Solar Salt and Hitec® fluids [10]. Also noteworthy is the study by Botejara-Antúnez et al. (2025), which analyzed new

fluids, such as Liquid Sodium, Lead-bismuth eutectic, Hitec XL® salt and Helisol® 5A silicone [56].

1.1. Novelty and objectives of research

The novelty of the current research lies in the analysis, per unit of heat transfer, of the cause-and-effect relationship that the life cycle of different low-melting point Molten Salts used in CSP plants with TES technology has on Human Health, Ecosystem Quality, and Resource Availability. It also includes the characterization and assessment of new salt formulations, by subjecting them to comparative assessment with traditional Molten Salts such as Solar Salt, Hitec® and Hitec XL®. Therefore, the research results will generate previously unavailable knowledge and thus expand scientific literature.

The objective, therefore, is to characterize new low-melting point Molten Salt formulations, assessing and comparing their environmental performance with traditional formulations as part of an initial pre-selection framework. To this end, the LCA tool is used to quantify the performance and identify the most suitable Molten Salts based on their impact. In this way, environmental dimensions can be added to the decision-making process of CSP plant managers, combining it with economic and technical factors to optimize their strategic selection.

2. Materials and methods

2.1. Molten salt characterization

The new molten salts investigated in this work were selected based on a comprehensive review of the existing scientific literature. Nine promising candidates were identified from this review for further experimental characterization. The primary selection criterion was a wide operational temperature window, defined as the difference between the onset of thermal degradation and the melting point. Salts exhibiting the broadest liquidus range as this property is critical for enhancing thermal energy storage capacity and operational flexibility in CSP applications. It should be noted that the thermophysical properties reported herein are initial values, which may evolve over time due to the decomposition processes of the molten salts. The nine selected salts and their respective chemical compositions are detailed in Table 1.

Table 1. *Chemical compositions of the new low-melting point salts studied in this work*

N#	$NaNO_3$ (%wt)	KNO_3 (%wt)	$Ca(NO_3)_2$ (%wt)	$LiNO_3$ (%wt)
Salt #1	10	60	10	20
Salt #2	-	60	10	30
Salt #3	20	60	10	10
Salt #4	-	59	32	9
Salt #5	18	52	-	30

Salt #6	28	52	-	20
Salt #7	15	43	42	-
Salt #8	46	-	19	35
Salt #9	33	22	29	16

The molten salt samples were prepared by first weighing the individual nitrate components (purities and suppliers listed in Table 2) according to the desired weight percentages for each composition. The weighed components were then combined in a sealed container and shaken to achieve a homogeneous mixture. To minimize moisture absorption, especially for hygroscopic salts such as $Ca(NO_3)_2$ and $LiNO_3$, the prepared mixtures were stored at room temperature (20-25 °C) in desiccators with silica gel for at least 24 h prior to characterization and were kept in tightly closed containers until immediately before each measurement. No additional drying or preheating was applied before testing, to reflect realistic industrial handling conditions. All samples were characterized within 48 hours after preparation to ensure consistency and minimize any potential degradation or moisture uptake over extended storage.

Table 2. Suppliers, purity, and impurity concentrations of the nitrates investigated in this work.

Nitrate	**Supplier**	**Purity (%)**	**Cl^- (ppm)**	**SO_4^{2-} (ppm)**
$NaNO_3$	Basf	99.5	60.8	> 20
KNO_3	Haifa	99-100	236.3	> 20
$LiNO_3$	Altichem sas	98	150	59.2
$Ca(NO_3)_2$	Krystalfeed calcio	98	> 100	36

The thermal stability of the samples was assessed by thermogravimetric analysis (TGA), with the degradation temperature defined as the point of a 3% mass loss. This analysis was conducted using an SDT Q600 instrument (TA Instruments). Samples were subjected to a dynamic heating regime from ambient temperature to 700 °C under a continuous air atmosphere at a flow rate of 50 mL/min to evaluate their thermal stability.

Thermal properties, including melting points, phase transitions, and specific heat capacity, were characterized using calorimetric techniques. Melting point and phase transition analyses were performed by Differential Scanning Calorimetry (DSC) on a DSC Q20 instrument (TA Instruments). Samples were subjected to a controlled thermal cycle under a constant nitrogen purge to ensure an inert atmosphere. The cycle consisted of heating the sample until complete melting was achieved, followed by cooling back to ambient temperature, with both steps conducted at a constant rate of 10 °C/min.

For a more detailed analysis of specific heat capacity (Cp), Modulated Differential Scanning Calorimetry (MDSC) was employed on the same instrument. This technique utilizes a superimposed sinusoidal heating rate on a conventional linear temperature ramp. The MDSC measurements were performed at a heating rate of 10 °C/min and under a constant nitrogen purge to ensure a controlled atmosphere for the molten salts. Prior to

the measurements, the instrument was calibrated and verified using a sapphire standard following the manufacturer's recommended procedure.

The density of the Molten Salt mixtures was experimentally determined using the Archimedean principle with a standard graduated densitometer. The methodology involved measuring the mass of a known volume of the sample. These measurements were subsequently taken at successive temperature intervals across the operational range. To guarantee thermal equilibrium and compositional homogeneity throughout the sample, the fluid was maintained at each target temperature for one hour prior to data acquisition. For this investigation, density was characterized over a temperature range from 200 °C to 450 °C. This approach facilitates the direct calculation of density (ρ, measured in g/cm^3) from the fundamental physical relationship, as seen in Equation 1.

$$\rho = \frac{m}{V} \quad (1)$$

Viscosity, a critical physicochemical property governing fluid dynamics and heat transfer efficiency, was thoroughly characterized. The measurements were conducted using a Discovery Hybrid Rheometer (DHR) from TA Instruments, equipped with a specialized high-temperature cell to facilitate analysis of molten salts. This instrument operates within a shear stress range of 20 to 150 nN·m with a resolution of 0.1 nN·m, achieving rotational velocities up to 300 rad/s and applying forces up to 50 N with a precision of 0.01 N. For each salt composition, viscosity was measured as a function of shear rate, which was systematically swept from 10 to 1000 s^{-1}, with data points recorded at discrete intervals. These experiments were performed at temperatures of 300, 350, 400, 425, and 450 °C; this range was selected based on the operational limits of the high-temperature cell and the thermal stability of the salts. The resulting shear stress (σ, in Pa) is intrinsically related to the dynamic viscosity (μ) and the applied shear rate (γ, in s^{-1}) through the fundamental constitutive equation for a Newtonian fluid, as defined in Equation 2.

$$\sigma = \mu * \gamma \quad (2)$$

Following the comprehensive experimental analysis detailed in the preceding methodology, the key physicochemical properties of the selected molten salt candidates have been quantified. A detailed presentation and discussion of the resultant data from all characterized salts are provided in the Supplementary Material, and the reader is referred to Fig. A1-A9 and Table A1-A2 for complete graphical representation and analysis.

2.2. Life Cycle Assessment (LCA)

To assess the environmental impact of Molten Salts, the Life Cycle Assessment (LCA) method was used to establish its processes and principles based on the regulatory framework of ISO 14040 [57] and ISO 14044 [58]. The environmental modeling and impact assessment were performed using SimaPro 10.1 software [59] together with the Ecoinvent 3.11 environmental database [60]. Primary data on the thermophysical characterization of the molten salts were obtained experimentally in this study, whereas background environmental processes and secondary inventory data were modeled using the Ecoinvent 3.11 dataset [61]. The ReCiPe 2016 assessment method [62], characterized

by providing a dual midpoint-endpoint perspective, was subsequently applied through 22 midpoint categories and 3 endpoint categories.

To combine the impact categories and compare them with each other and with other methods, a common reference unit was used: specific points, hereafter abbreviated as Pt. The impact indicators of the ReCiPe method are called "impact categories" in the midpoint approach; see Table 3.

Table 3. *ReCiPe 2016 impact categories.*

Impact Category	Acronym
Global warming, Human health	GWHH
Stratospheric Ozone depletion	SODP
Ionizing Radiation	IR
Ozone formation, Human health	OFHH
Fine particulate matter formation	FPMF
Human carcinogenic toxicity	HCT
Human non-carcinogenic toxicity	HnCT
Water consumption, Human health	WCHH
Global warming, Terrestrial ecosystems	GWTE
Global warming, Freshwater ecosystems	GWFE
Ozone formation, Terrestrial ecosystem	OFTE
Terrestrial acidification	TA
Freshwater eutrophication	FE
Marine eutrophication	ME
Terrestrial ecotoxicity	TE
Freshwater ecotoxicity	FEC
Marine ecotoxicity	MEC
Land use	LU
Water consumption, Terrestrial ecosystems	WCTE
Water consumption, Aquatic ecosystems	WCAE
Mineral resource scarcity	MRS
Fossil resource scarcity	FRS

The endpoint approach groups together the impact categories of the midpoint approach by damage pathways based on characterization factors. Thus, the three indicators, called "protection areas", are formed: Human Health, Resource Availability, and Ecosystem Quality. The unit for Human Health is DALY (Disability-Adjusted Life Years) and represents the years of life lost by a person due to illness. Resource Availability represents the additional cost of extracting resources in the future (expressed in US$). Finally, Ecosystem Quality reflects the impact of the midpoints on the environment, and the unit is the species' loss per unit of time (species·yr).

2.3. Case study description

An environmental analysis of different low-melting point Molten Salts was carried out for their potential application as Thermal Energy Storage (TES) systems in CSP plants. For this purpose, up to 7 plants and/or facilities in the EUROACE region (Spain-Portugal) were considered as representative operational references, given the strategic relevance of the Iberian Peninsula in the deployment of CSP technology, specifically those located in

the provinces of Badajoz and Évora [63]. The salts analyzed included those most commonly used in the aforementioned CSP plants (Solar Salt, Hitec®, and Hitec XL®), as well as nine new salt formulations whose composition and technical characteristics have been described in previous sections (see Table 1). However, no plant-specific operational or environmental data from these facilities were directly incorporated into the LCA model. A techno-economic analysis was also performed.

An LCA was carried out for the 12 most promising and representative Molten Salt formulations for CSP technology globally, first verifying that they met the minimum specifications and/or requirements established for specific heat (c_p), density (ρ), thermal conductivity (λ) and dynamic viscosity (μ). To this end, a wide variety of scientific literature was consulted [6,64], the validity of which was verified by an international panel of expert researchers with a combined experience of over 150 years in the area of energy storage engineering.

Table 4 details the technical specifications of each of the Molten Salts under study (Solar Salt, Hitec®, Hitec XL®, and the nine new salt formulations), describing their thermophysical properties at a common operating temperature of 300°C (typical operating temperature), where all the salts were thermally stable [65].

Table 4. *Technical specifications of heat transfer fluids.*

Molten Salt*	***Cost (€/kg)***	***Melting Point (ºC)***	***Degradation temperature (ºC)***	***Working range (ºC)***	***Properties at 300ºC***			
					c_p (J/g·ºC)	***ρ (g/cm³)***	***λ (W/m·K)***	***μ (mPa·s)***
Solar Salt [64,66]	0.53	227	597	370	1.50	1.90	0.50	3.27
Hitec® [64,66]	0.88	140	530	390	1.56	1.86	0.40	3.36
Hitec XL® [64,66]	1.13	130	550	420	1.44	1.99	0.52	6.37
Salt #1 [66,67]	2.08	209	588	379	2.40	2.20	0.96	19.36
Salt #2 [66,68]	2.80	192	592	400	2.60	2.30	1.09	17.96
Salt #3 [66,67]	1.36	131	601	469	1.70	2.25	0.69	19.02
Salt #4 [66,69]	1.28	207	567	360	3.30	2.30	1.38	23.07
Salt #5 [66,70]	2.36	116	585	469	3.25	2.06	1.21	13.73
Salt #6 [66,71,72]	2.04	130	592	462	2.00	2.15	0.78	15.49
Salt #7 [66,73,74]	0.54	185	609	424	3.50	2.31	1.47	20.87
Salt #8	2.82	195	566	371	3.00	2.18	1.19	17.82

[66,69]								
Salt #9 [66,69]	1.57	197	593	396	3.30	2.27	1.36	16.33

* Thermophysical properties were validated based on the cited references for each molten salt

2.4. Life Cycle Inventory (LCI)

In their application as TES systems in CSP plants, Molten Salts play a fundamental role in self-regulated energy generation management, by providing the necessary thermal energy for steam production.

In this context, the specific heat (c_p) of Solar Salt is a key parameter in heat transfer processes, as it determines the capacity of a material to absorb and/or release heat. This property, commonly known as sensible heat (Q), is directly related to the thermal energy exchanged by salt as a result of temperature variations, and its behavior is mathematically described in Equation 3.

$$Q = m \times c_p \times \Delta T \quad (3)$$

Where m is the mass of the storage material and ΔT is the temperature change that occurs during the process.

Therefore, in an objective assessment of the saline solutions in the case study as TES systems, it is essential to establish the heat transfer unit, i.e., 1 MJ, as the functional unit. Thus, the different requirements for raw materials, energy, and transportation per unit of heat transfer of Molten Salt were considered, establishing the Spanish energy matrix as the energy mix. Furthermore, the "cradle to grave" time model, based on the traditional economic model of product lifespan [75], was adopted, using a time period of 25 years [76,77].

The system boundaries included raw material extraction and production, molten salt manufacturing, transportation processes, operational use associated with the functional unit, and end-of-life transport and waste management stages. Infrastructure processes associated with CSP plant construction were excluded from the assessment because they contributed equally across the molten salt formulations evaluated. Likewise, recycling pathways and operational salt replenishment were excluded due to current uncertainty associated with large-scale recovery processes and representative long-term replacement rates for degraded CSP molten salts [78,79]. Minor material and energy flows that make negligible contributions to the overall environmental impact were also excluded, following conventional cut-off criteria commonly adopted in LCA studies [75].

In accordance with Equation 3 [80], the mass normalization was performed using a representative ΔT of 260 °C, consistent with the typical working ranges employed in molten-salt TES systems in CSP plants [81].

Table 5 presents the Life Cycle Inventory (LCI) of the Molten Salts under study, normalized per unit of heat transfer.

Table 5. *Life cycle inventory of Molten Salts to be analyzed.*

Molten Salt	Weight (kg)	*Compounds (kg)*					*Transport (km)*	
		$NaNO_3$	KNO_3	$NaNO_2$	$Ca(NO_3)_2$	$LiNO_3$	*Raw materials*	*Waste*
Solar Salt	2.56	1.54	1.02	-	-	-	200	50
Hitec®	2.49	0.17	1.32	1.00	-	-	200	50
Hitec XL®	2.70	0.19	1.22	-	1.29	-	300	50
Salt #1	1.62	0.16	0.97	-	0.16	0.33	500	150
Salt #2	1.39	-	0.83	-	0.14	0.42	500	150
Salt #3	2.29	0.46	1.37	-	0.23	0.23	500	150
Salt #4	1.11	-	0.65	-	0.36	0.10	500	150
Salt #5	1.22	0.22	0.64	-	-	0.36	400	150
Salt #6	1.95	0.54	1.02	-	-	0.39	400	150
Salt #7	1.11	0.16	0.47	-	0.48	-	300	50
Salt #8	1.30	0.60	-	-	0.25	0.45	500	150
Salt #9	1.18	0.39	0.26	-	0.34	0.19	500	150

In accordance with Spanish waste-management regulations, a distance of 50 km was considered from the CSP plant to the end-of-life waste-management point, with 150 km used for nitrates that required special management processes [82]. Raw-material transport distances were estimated using representative industrial supply-chain scenarios for CSP facilities in the Iberian Peninsula, accounting for the limited commercial availability and specialized handling requirements of certain nitrate-based compounds. Furthermore, a sensitivity analysis of the transport distances was conducted to mitigate potential inconsistencies and subjectivity associated with these assumptions (see Table 8 and Fig. 6). Trucks ranging from 16 to 32 tons, manufactured and registered after October 2008, were used. Consequently, transport emissions were classified as EURO5, with emission values of 1.50, 0.46, and 2.00 g/kWh for CO, hydrocarbons, and NO_x [83].

3. Results

3.1. Molten salt characterization

DSC analysis revealed that most novel salt formulations exhibit melting points within the range of 128 to 250 °C, with several compositions showing promising low-temperature behavior. Salt #5 (18 wt% $NaNO_3$ - 52 wt% KNO_3 - 30 wt% $LiNO_3$) displayed the lowest melting point at 128 °C, consistent with its ternary eutectic nature, while Salt #3 required complete melting at 250 °C, indicating a partially solid region between 130 and 250 °C. Solid–solid phase transitions associated with KNO_3 were observed around 130-134 °C across several compositions. Notably, Salt #7 (calcium-sodium-potassium ternary eutectic) showed a melting point of 187 °C instead of the expected 120 °C, which is attributed to the presence of calcium nitrate tetrahydrate without prior drying, reflecting

realistic industrial handling. The highest enthalpy of fusion was recorded for Salt #8 (183.5 J/g at 183.65 °C), indicating a strong capacity for absorbing thermal energy. Full thermograms and individual values are available in the Supplementary Material (Fig. A1–A3).

TGA analysis showed degradation temperatures (3% mass loss) ranging from approximately 550 to 612 °C across the nine novel salts. Salt #6 exhibited the highest thermal stability (degradation at 611.9 °C), followed closely by Salt #3 (601.5 °C) and Salt #2 (596.0 °C), all without significant mass gains prior to decomposition. Salt #5, the ternary eutectic ($NaNO_3$ - KNO_3 - $LiNO_3$), degraded at 580.8 °C with a linear profile and no oxide formation, confirming its reliability. In contrast, calcium-rich compositions (Salts #7, #8, and #9) showed lower stability: Salt #7 lost 15 % mass due to water evaporation below 200 °C and gained 10 % mass above 450 °C due to oxide/carbonate formation, degrading at ~550 °C; Salt #8 exhibited a mass gain exceeding 20 % before degrading at 553.3 °C, indicating poor oxidative resilience; Salt #9 degraded at 595.4 °C but showed a 10 % initial mass loss from moisture and progressive oxidation above 500 °C. Several salts (e.g., Salt #1) displayed a 5-6 % mass gain between 180-220 °C attributed to calcium oxide/carbonate formation. Overall, Li-containing eutectic compositions (Salts #5 and #6) demonstrate superior thermal stability, whereas calcium nitrate tetrahydrate-based salts require drying or inert atmospheres for high-temperature CSP operation. Full TGA thermograms are provided in the Supplementary Material (Figs. A4–A6).

Specific heat capacity values at 300 °C are reported relative to Solar Salt (1.495 J/g°C). The novel salts exhibited corrected Cp values ranging from approximately 2.0 to 3.7 J/g°C, substantially exceeding the benchmark. Salt #7 showed the highest corrected Cp (3.706 J/g°C), followed by Salt #4 (3.535 J/g°C), Salt #9 (3.324 J/g°C), Salt #5 (3.237 J/g°C), and Salt #8 (3.186 J/g°C). Salt #1, #2, and #3 yielded corrected values of 2.398, 2.863, and 2.006 J/g°C, respectively, while Salt #6 gave 2.158 J/g°C. Consistent with the literature, higher $LiNO_3$ content generally increased C_p, as observed for Salts #2, # 5, #7, and #8. Notably, Salt #4 (with moderate $LiNO_3$ but higher $Ca(NO_3)_2$) and Salt #9 (quaternary mixture with 16 wt% $LiNO_3$) achieved exceptionally high values, suggesting synergistic effects among multiple cations beyond a simple $LiNO_3$ dependence. Full C_p curves and raw data are available in the Supplementary Material (Figs. A7–A9).

The results of density and viscosity measurements are extensively presented and discussed in the Supplementary Material. The key numerical values are summarized in Table A1 and A2 (Supplementary Material).

3.2. Life Cycle Assessment

A dual midpoint-endpoint approach based on the ReCiPe 2016 was used to determine which processes had the greatest influence on environmental impacts. To do this, the results obtained were characterized, normalized, and weighted so as to establish a comparative framework and determine which impact categories or protection areas presented the most unfavorable results [84,85]. Fig. A10, presented in the Supplementary

Material, provides an overview of the two impact assessment approaches employed in this study, in accordance with the specifications of ISO 14044 [58].

Table 6 presents the LCA results by impact category for each of the Molten Salts studied.

Table 6. *LCA results by impact category*

Impact Categories	*Solar Salt*	*Hitec®*	*Hitec XL®*	*Salt #1*	*Salt #2*	*Salt #3*	*Salt #4*	*Salt #5*	*Salt #6*	*Salt #7*	*Salt #8*	*Salt #9*
***GW_T (kg CO_2 eq)**	10.0	7.3	8.7	4.1	3.0	6.7	2.9	3.0	5.6	3.6	4.1	3.9
SODP (kg CFC_{11} eq)	$1.7\cdot10^{-4}$	$9.2\cdot10^{-5}$	$1.8\cdot10^{-4}$	$8.1\cdot10^{-5}$	$5.9\cdot10^{-5}$	$1.3\cdot10^{-4}$	$6.4\cdot10^{-5}$	$5.3\cdot10^{-5}$	$1.0\cdot10^{-4}$	$7.4\cdot10^{-5}$	$6.2\cdot10^{-5}$	$6.8\cdot10^{-5}$
IR (kBq Co-60 eq)	0.4	0.4	0.2	0.1	$6.2\cdot10^{-2}$	0.2	$5.5\cdot10^{-2}$	$9.0\cdot10^{-2}$	0.2	$8.8\cdot10^{-2}$	0.2	0.1
OFHH (kg NO_x eq)	$1.8\cdot10^{-2}$	$1.6\cdot10^{-2}$	$1.5\cdot10^{-2}$	$7.3\cdot10^{-3}$	$5.3\cdot10^{-3}$	$1.2\cdot10^{-2}$	$5.3\cdot10^{-3}$	$5.3\cdot10^{-3}$	$9.8\cdot10^{-3}$	$6.3\cdot10^{-3}$	$6.9\cdot10^{-3}$	$6.7\cdot10^{-3}$
FPMF (kg PM2.5 eq)	$1.0\cdot10^{-2}$	$9.5\cdot10^{-3}$	$8.0\cdot10^{-3}$	$3.8\cdot10^{-3}$	$2.7\cdot10^{-3}$	$6.3\cdot10^{-3}$	$2.6\cdot10^{-3}$	$2.9\cdot10^{-3}$	$5.3\cdot10^{-3}$	$3.3\cdot10^{-3}$	$4.1\cdot10^{-3}$	$3.7\cdot10^{-3}$
OFTE (kg NOx eq)	$1.8\cdot10^{-2}$	$1.6\cdot10^{-2}$	$1.6\cdot10^{-2}$	$7.4\cdot10^{-3}$	$5.4\cdot10^{-3}$	$1.2\cdot10^{-2}$	$5.3\cdot10^{-3}$	$5.4\cdot10^{-3}$	$1.0\cdot10^{-2}$	$6.4\cdot10^{-3}$	$7.0\cdot10^{-3}$	$6.7\cdot10^{-3}$
TA (kg SO_2 eq)	$3.2\cdot10^{-2}$	$2.6\cdot10^{-2}$	$2.8\cdot10^{-2}$	$1.3\cdot10^{-2}$	$9.3\cdot10^{-3}$	$2.1\cdot10^{-2}$	$9.5\cdot10^{-3}$	$9.5\cdot10^{-3}$	$1.8\cdot10^{-2}$	$1.1\cdot10^{-2}$	$1.3\cdot10^{-2}$	$1.2\cdot10^{-2}$
FE (kg P eq)	$2.0\cdot10^{-3}$	$2.0\cdot10^{-3}$	$1.5\cdot10^{-3}$	$7.6\cdot10^{-4}$	$5.5\cdot10^{-4}$	$1.2\cdot10^{-3}$	$4.9\cdot10^{-4}$	$6.1\cdot10^{-4}$	$1.1\cdot10^{-3}$	$6.2\cdot10^{-4}$	$9.5\cdot10^{-4}$	$7.8\cdot10^{-4}$
ME (kg N eq)	$6.0\cdot10^{-3}$	$1.3\cdot10^{-3}$	$1.6\cdot10^{-3}$	$6.4\cdot10^{-4}$	$3.1\cdot10^{-5}$	$1.8\cdot10^{-3}$	$2.7\cdot10^{-5}$	$8.5\cdot10^{-4}$	$2.1\cdot10^{-3}$	$6.5\cdot10^{-4}$	$2.3\cdot10^{-3}$	$1.5\cdot10^{-3}$
TE (kg 1.4 DCB eq)	30.7	23.8	27.0	13.6	10.6	21.1	9.4	10.5	18.4	11.1	14.9	12.8
FEC (kg 1.4 DCB eq)	0.2	0.2	0.2	0.1	$8.0\cdot10^{-2}$	0.2	$7.1\cdot10^{-2}$	$7.8\cdot10^{-2}$	0.1	$8.3\cdot10^{-2}$	0.1	$9.5\cdot10^{-2}$
MEC (kg 1.4 DCB eq)	0.3	0.3	0.3	0.1	0.1	0.2	0.1	0.1	0.2	0.1	0.2	0.1
HCT (kg 1.4 DCB eq)	0.2	0.2	0.2	$8.0\cdot10^{-2}$	$6.1\cdot10^{-2}$	0.1	$5.3\cdot10^{-2}$	$6.4\cdot10^{-2}$	0.1	$6.5\cdot10^{-2}$	$9.4\cdot10^{-2}$	$7.7\cdot10^{-2}$
HnCT (kg 1.4 DCB eq)	7.3	5.9	6.9	3.5	2.8	5.3	2.5	2.7	4.6	2.8	3.7	3.2
LU (m^2a crop eq)	0.1	0.1	0.1	$5.5\cdot10^{-2}$	$4.3\cdot10^{-2}$	$8.3\cdot10^{-2}$	$3.7\cdot10^{-2}$	$4.2\cdot10^{-2}$	$7.3\cdot10^{-2}$	$4.2\cdot10^{-2}$	$5.2\cdot10^{-2}$	$4.8\cdot10^{-2}$
MRS (kg Cu eq)	$4.1\cdot10^{-2}$	$2.8\cdot10^{-2}$	$4.1\cdot10^{-2}$	0.2	0.2	0.1	$6.4\cdot10^{-2}$	0.2	0.2	$1.7\cdot10^{-2}$	0.2	0.1
FRS (kg oil eq)	1.6	1.5	1.2	0.6	0.4	1.0	0.4	0.5	0.9	0.5	0.6	0.6
****WC_T (m^3)**	$9.2\cdot10^{-2}$	0.1	$6.9\cdot10^{-2}$	$2.4\cdot10^{-2}$	$1.2\cdot10^{-2}$	$4.9\cdot10^{-2}$	$1.9\cdot10^{-2}$	$1.7\cdot10^{-2}$	$3.9\cdot10^{-2}$	$2.8\cdot10^{-2}$	$3.1\cdot10^{-2}$	$3.0\cdot10^{-2}$

**WC_T = WCHH + WCTE + WCAE

*GW_T = GWHH + GWTE + GWFE

It can be observed that Solar Salt is the least favorable, presenting the maximum scores in 13 of 18 impact categories and with values between 1.84 and 5.02 times greater than the mean environmental impact associated with the other salts analyzed.

Fig. 1 shows the results of the impact category characterization process. Thus, for this initial approach, the least favorable impact category in terms of DALY score was GWHH, in which Solar Salt stands out with an impact of $9.40\cdot10^{-6}$ DALY. Regarding the overall ecosystem quality, Solar Salt again stood out from the other Molten Salts analyzed, generating the greatest impacts in the GWTE category ($2.83\cdot10^{-8}$ species·yr). Finally, for the characterization of the resource scarcity, Solar Salt again presented the highest score, generating the greatest impact in the FRS category (0.53 US$).

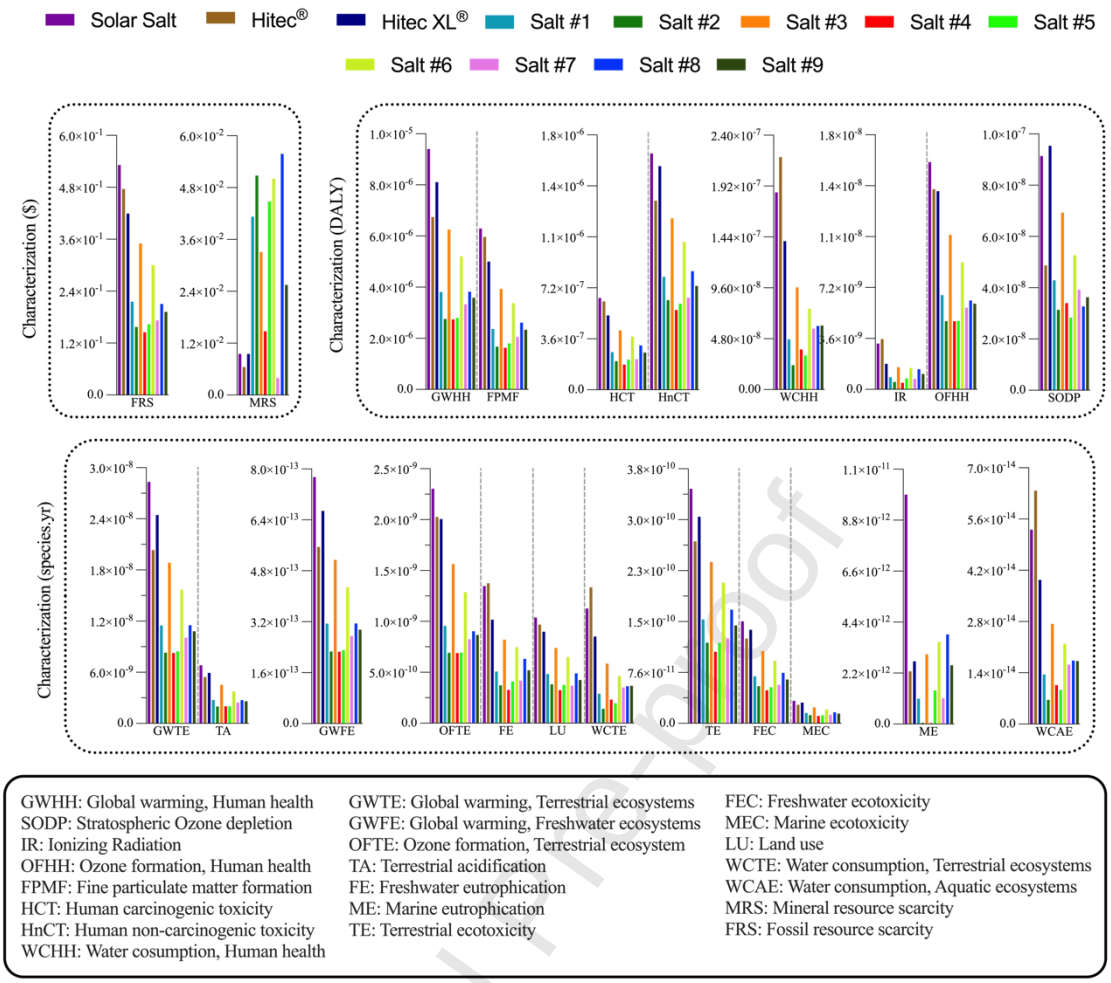

Fig. 1. *ReCiPe 2016 characterization for midpoint impact categories.*

Fig. 2 shows the results of the internal normalization process. For visualization purposes, the value of 100% was assigned to the system with the highest score in each category. The proportion of the impact of the remaining systems was established from this rescaling process. Thus, analyzed by impact category, Solar Salt, Hitec®, Hitec XL®, Salt #5, and Salt #8 presented the highest values in the different impact categories. Salts #5 and #8 presented the highest values in the MRS category; Hitec XL® in the SODP category; Hitec® in the IR, WCHH, FE, WCTE, and WCAE categories; and Solar Salt in the remaining impact categories (15 out of 22 categories). In general, the other Molten Salts presented similar values of relative importance in each impact category.

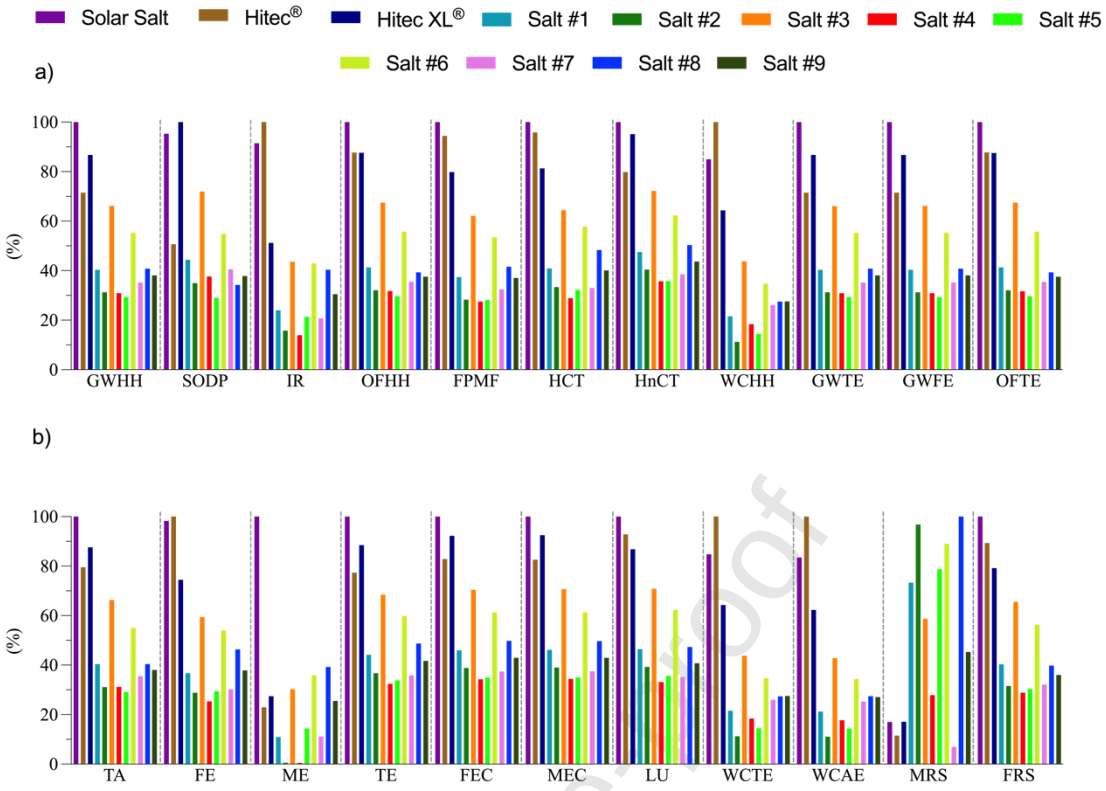

Fig. 2. *ReCiPe 2016 internal normalization for midpoint impact categories.*

3.3. Results according to midpoint approach

Fig. 3 shows the single-score results after applying weights to the midpoint impact categories. The GWHH, FPMF, and HnCT categories can be observed to be those that presented the highest values.

Solar Salt stands out as the most harmful to the environment when all categories are considered. The most significant categories are (in descending order): GWHH (158.29 mPt), FPMF (106.04 mPt), HnCT (28.13 mPt), GWTE (15.82 mPt), HCT (10.93 mPt) and TA (3.81 mPt). Hitec XL®, Hitec® and Salt #3 follow, with absolute impacts of 283.49, 273.00 and 220.03 mPt, respectively.

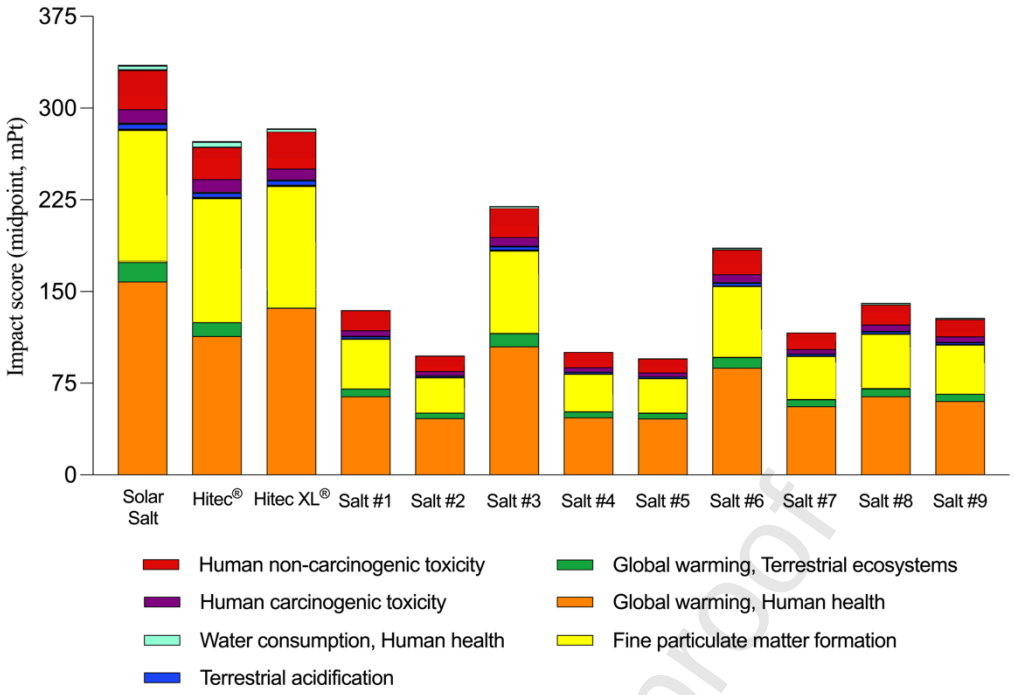

Fig. 3. *Impact analysis – Single score midpoint results.*

3.4. Results according to endpoint approach

Fig. 4 shows the assessment of damage by protection area as an intermediate step towards obtaining the single score in the endpoint approach. Regarding the damage to the Human Health, the Solar Salt value ($1.8 \cdot 10^{-5}$ DALY) was 2.08 times higher than the mean of the other saline solutions. This was followed by Hitec XL® salt, with $1.6 \cdot 10^{-5}$ DALY, and in third place, Hitec® salt, with $1.5 \cdot 10^{-5}$ DALY. As for the damage to the Ecosystems Quality, the Solar Salt value ($4.2 \cdot 10^{-8}$ species·yr) was 2.10 times higher than the mean of the other saline solutions. This was followed by Hitec XL®, Hitec® and #3 salts, with very close values ($3.6 \cdot 10^{-8}$, $3.2 \cdot 10^{-8}$ and $2.8 \cdot 10^{-8}$ species·yr, respectively). Finally, Solar Salt again had the greatest impact on resource availability (0.54 US$), with a value 1.90 times higher than the means of the other saline solutions. It was followed by Hitec®, Hitec XL® and #3 salts, with impacts of 0.48, 0.43 and 0.38 US$, respectively.

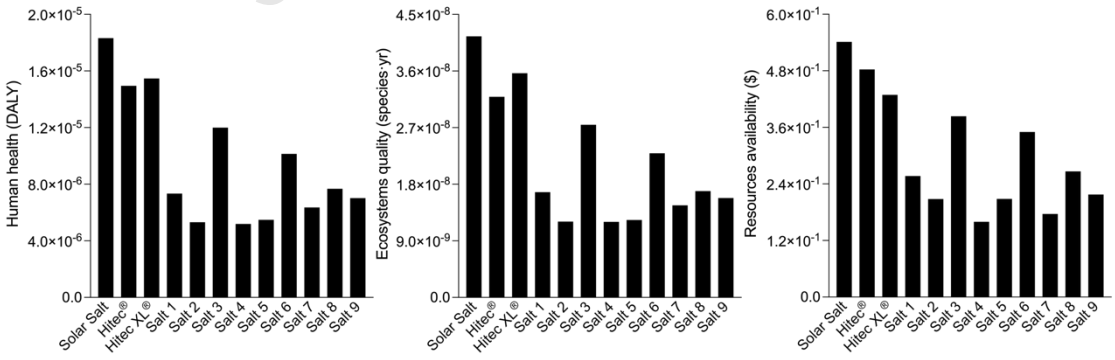

Fig. 4. *Damage assessment by protection areas.*

Fig. 5 shows the results under the endpoint approach for each of the Molten Salts studied after normalizing and weighing the characterization factors. This allows for a comparison

of the different saline solutions by aggregating the impacts in the protection areas. Thus, it can be observed that the least favorable Molten Salt is Solar Salt, since it has an impact of 335.44 mPt, of which 308.39 mPt are attributable to the Human Health protection area (HH, 92.0%), 23.19 mPt to the Ecosystems Quality protection area (EQ, 6.9%) and 3.86 mPt to the Resources Availability protection area (RA, 1.1%). Salt #5 presents the most desirable environmental impact (95.29 mPt), 3.52 times lower than the Solar Salt impact. Salts #2 and #4 closely follow, with 97.74 and 100.66 mPt, respectively. Finally, it can be seen how the Resources Availability (RA) protection area had hardly any impact.

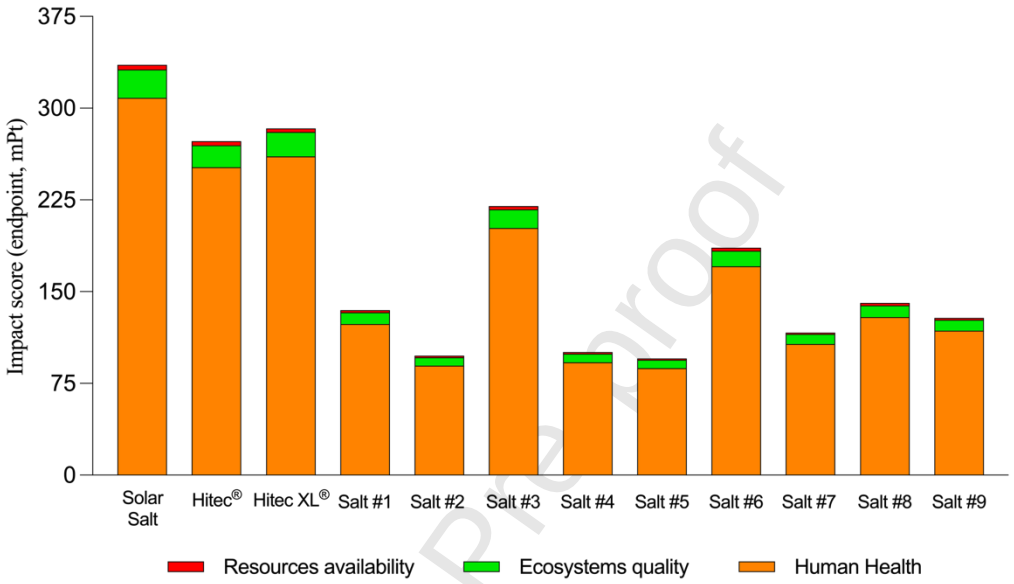

Fig. 5. *Impact analysis - Single score endpoint results.*

3.5. Sensitivity analysis

An exhaustive sensitivity analysis was conducted, considering variations in key parameters that affect the LCA results, including transportation distances, specific heat capacity (C_p), energy mix, and $LiNO_3$ environmental burdens. This analysis allowed the influence of these assumptions on the environmental performance of the molten salts to be quantified. Table 7 summarizes the alternative scenarios considered in the sensitivity analysis.

Table 7. *Case studies included in the sensitivity analysis*

Key parameter	*Case study*	*Sub-case*	*Description*
Baseline	C_0	-	The baseline case study is defined in the methodology section
Transportation distances	C_I	$C_{I\text{-}I}$	1,000 % supply distance for raw materials increment
		$C_{I\text{-}II}$	1,000 % waste disposal distance increment
C_p	C_{II}	$C_{II\text{-}I}$	10% specific heat capacity increment
		$C_{II\text{-}III}$	10% specific heat capacity reduction
Energy mix	C_{III}	-	100% renewable electricity mix scenario
$LiNO_3$ environmental burdens	C_{IV}	$C_{IV\text{-}I}$	10% $LiNO_3$ environmental burden increment
		$C_{IV\text{-}II}$	10% $LiNO_3$ environmental burden reduction

Table 8 and Fig. 6 summarize and illustrate the results derived from the sensitivity analysis of key parameters in the LCA.

Table 8. *Sensitivity analysis results*

Case study	*Sub-case*	*Moltens Salts environmental impacts (mPt)*											
		Solar Salt	***Hitec®***	***Hitec XL®***	***Salt #1***	***Salt #2***	***Salt #3***	***Salt #4***	***Salt #5***	***Salt #6***	***Salt #7***	***Salt #8***	***Salt #9***
C_0	-	335.44	272.99	283.49	134.78	97.74	220.03	100.66	95.29	186.02	116.55	140.66	128.57
C_I	$C_{I\text{-}I}$	362.90	299.70	312.45	152.16	112.65	244.59	113.75	107.20	206.93	128.45	154.60	141.23
	$C_{I\text{-}II}$	356.04	293.03	305.21	147.81	108.92	238.45	110.48	104.22	201.70	125.48	151.11	138.07
C_{II}	$C_{II\text{-}I}$	305.44	245.73	254.95	121.21	87.81	197.62	86.55	85.76	166.77	104.89	126.10	115.45
	$C_{II\text{-}II}$	373.31	300.34	311.60	148.15	107.32	241.53	105.78	104.82	203.83	128.20	154.13	141.10
C_{III}	-	301.90	237.51	266.48	129.39	86.99	209.02	93.62	84.81	174.85	101.40	123.78	110.57
C_{IV}	$C_{IV\text{-}I}$	335.44	272.99	283.49	123.26	91.24	201.92	91.90	89.97	168.92	116.55	134.51	118.93
	$C_{IV\text{-}II}$	335.44	272.99	283.49	146.30	116.63	236.31	111.36	98.16	203.11	116.55	148.17	136.96

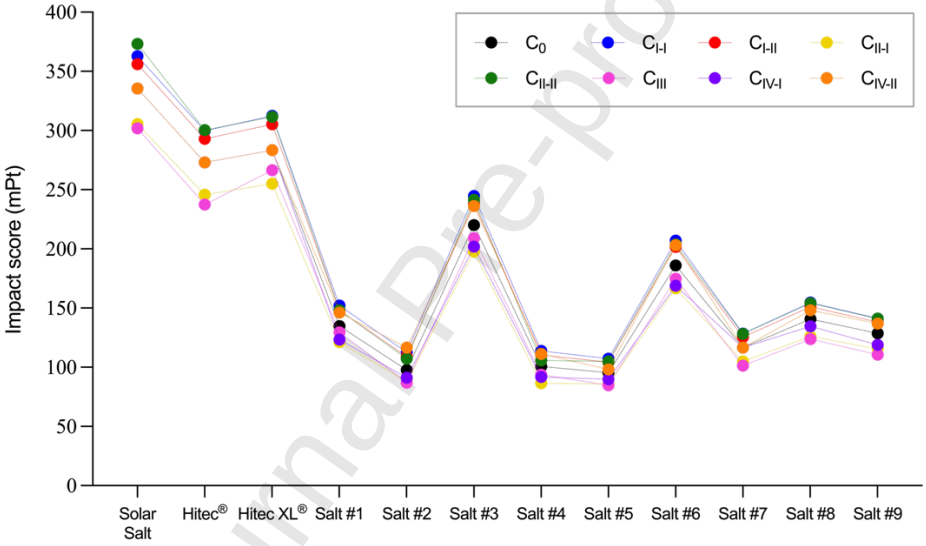

Fig. 6. *Sensitivity analysis of LCA key parameters*

4. Discussion

Among the molten salt formulations analyzed, Salt #5 and Salt #7 exhibited the most favorable combination of thermophysical properties for application as thermal storage and heat transfer media in CSP systems. Both salts demonstrate a high specific heat capacity, 3.24 and 3.58 J/g°C respectively, significantly exceeding that of the benchmark Solar Salt. This enhancement implies a greater thermal energy storage capability per unit mass, which directly translates into improved plant efficiency and reduced material requirements for energy storage [86].

In addition to their superior Cp values, these two formulations exhibit broad working ranges of 469 °C and 496 °C, ensuring stability over a wide operational temperature window. This thermal resilience is particularly advantageous for high-temperature CSP systems, as it minimizes the risk of salt degradation or solidification during cyclic operation. Furthermore, both compositions maintain relatively low viscosities compared with other mixtures tested.

Overall, the combination of high specific heat, wide working temperature range, and acceptable viscosity identifies Salt #5 and Salt #7 as the most promising candidates for advanced thermal energy storage applications. Their balanced behavior between energy density, thermal stability, and fluidity supports their selection for further optimization and long-term performance evaluation within this research. However, it was essential to contrast these preliminary results through an analysis of their environmental performance to ensure a comprehensive assessment of their overall viability [56,87].

From the environmental dimension, the LCA carried out has made it possible to identify the most relevant areas of damage. Of the three areas assessed -Human Health, Ecosystems Quality and Resources Availability-, the results show that the environmental impact of Molten Salts is primarily associated with Human Health area. This trend is observed in all the proposed saline solutions, with an average contribution of 91.84%. Ecosystems Quality area has a smaller impact, of 6.88%. Finally, the environmental impact associated with Resources Availability is not significant (1.28%).

Analyzing the harmonized environmental scoring criteria at the midpoint level reveals a common trend across all Solar Salts. The environmental impact associated with the categories Global warming Human health (GWHH), Fine particulate matter formation (FPMF), and Human non-carcinogenic toxicity (HnCT) averages 47.19%, 31.61%, and 8.38%, respectively. Taken together, the three categories average 87.18%, which represents 94.84% of the impact associated with the final human health scoring criterion. This impact stems primarily from the production process of the various salt solutions (with a mean weight of 68.53%), while the impact associated with the different transport processes considered throughout the life cycle is relatively insignificant (1.91%).

The addition of lithium nitrate ($LiNO_3$) to Molten Salts increases their price (between 1.65 and 3.66 €/kg) [88]. However, it significantly reduces their characteristic environmental impact, which results in scores between 16.9 and 46.3% lower than those of traditional Solar Salt, Hitec® and Hitec XL® (131.03, 109.64 and 105.01, respectively) per kg of Molten Salt (see Fig. A11 and Fig. A12 in the Supplementary Material). Of these salts, Salt #2 and Salt #5 stand out as being the most favorable compositions per kg of Molten Salt (70.32 and 82.51 mPt, respectively), up to 1.44 times more favorable than the mean and up to 1.86 times more favorable than Solar Salt.

In their application as TES systems for CSP plants and closely related to the observed increase in thermal conductivity, the Molten Salts that incorporate lithium nitrate show even greater reductions in environmental impact, ranging from 34.41 to 71.59%. This improvement is mainly attributed to the higher thermal efficiency of the mixtures [89], which offsets the additional environmental burdens associated with $LiNO_3$ extraction and conversion processes considered in the LCA model. This allowed for the same amount of energy transferred (1 MJ) to be achieved using a smaller mass of salt (see Table 5), thereby reducing environmental impacts per functional unit.

In this context, Salt #5 stands out as the most favorable composition (95.29 mPt), up to 1.82 times more favorable than the mean and up to 3.52 times more favorable than Solar Salt. Furthermore, this saline solution requires only 1.22 kg of salt to achieve said functional unit, with an associated cost of 2.88 €/MJ (value very close to the estimated average cost of 2.61 €/MJ). This cost is feasible, despite being double that of Solar Salt

(1.36 €/MJ). Therefore, it is presented as a promising saline solution, particularly from an environmental and material-efficiency perspective, while maintaining economic viability. However, it should be noted that the advantages of Salt #5 depend on the availability of $LiNO_3$, whose supply is geographically concentrated and potentially sensitive to market constraints.

Additionally, the incorporation of LiNO3 has improved the thermo-physical properties of the compositions, reducing their melting point to ~129°C (compared to the 227°C for Solar Salt), which allows to operate at lower temperatures and with lower energy requirements [23]. Likewise, an increase in thermal conductivity is observed, with values ranging from 0.78 to 1.38 W/m·K, which could contribute to improved heat-transfer performance and thermal efficiency under real CSP operating conditions [90].

The results obtained in the present research are aligned with those obtained by other authors, such as Batuecas et al. (2017), in previous studies [10]. Thus, it can be observed that in both studies, the impact values of Solar Salt are the least favourable among all the Molten Salts assessed. Furthermore, the results obtained for Solar Salt, Hitec® and Hitec XL® (131.03, 109.64 and 105.01 mPt) are consistent with those obtained by Botejara et al. (2025) in their comparative LCA per kg of HTF from CSP plants [56]. However, the present study provides additional knowledge through the examination of new saline solutions that incorporate varying amounts of lithium nitrate ($LiNO_3$) in their formulations, resulting in significant reductions in their environmental impact scores (up to 46.34% per kg of Molten Salt and up to 71.59% per unit of heat transfer). Additionally, the application of the salts analyzed as TES media was assessed to characterize their performance, thus adding value through the standardized quantification of impacts per unit of heat transfer.

From an analytical perspective, it can be observed that the present study used a more comprehensive and up-to-date impact assessment method than those used in previous studies, namely ReCiPe 2016 [62], which covers the entire life cycle, thus obtaining overall results and allowing for the comparison at the midpoint and endpoint levels with other potential research [91]. This method, also used by Botejara et al. (2025), has 22 midpoint impact categories, in comparison to the 9 categories of the CML-IA method used by Batuecas et al. (2017) [92]. Additionally, it includes an endpoint analytical approach that classifies and groups the environmental impact results obtained in the midpoint approach by area of damage, which allows for a greater understanding of the damage pathways used and the scores obtained. Finally, the environmental database used in all the studies is the same, Ecoinvent, although the most up-to-date version is the one used in the present study (Ecoinvent 3.11 vs. Ecoinvent 3.8 and Ecoinvent 3.0) [60].

It is worth noting that the methodology used in this research offers several additional advantages. Adopting the “cradle to grave” approach provides a representative assessment framework for the main life-cycle stages considered in the present study, from raw material extraction to final disposal under the defined modeling assumptions, thereby facilitating detailed comparisons between processes or technological alternatives [93]. Furthermore, ReCiPe 2016 exhibits a remarkable versatility, which allows for its implementation in various life cycle assessment contexts [94], including the comparative environmental assessment of next-generation Molten Salt production processes.

Any adaptation of the study to be used in another country could lead to slight variations in the environmental impact results obtained due to modifications in the production processes and the country's energy mix [95], with the Spanish energy mix being the one used in the present study. However, the uncertainty and sensitivity of this research were minimized through various decisions based on a panel of qualified experts. Furthermore, a sensitivity analysis of key LCA parameters was conducted to evaluate the robustness of the results. The case studies evaluated (C_I–C_{IV}) produced variations in the overall environmental scores ranging from -14.0% to +19.3% relative to the baseline case study (C_0), with the greatest variability associated with the specific heat capacity (C_p) sub-cases due to their direct influence on mass normalization ($C_{II\text{-}I}$ and $C_{II\text{-}II}$, -14.0% to +11.3%, respectively). Despite these variations, the comparative ranking of the Molten Salts remained largely stable. Only minor changes were observed among intermediate-ranking $LiNO_3$-based formulations under the $LiNO_3$ environmental burden sub-cases ($C_{IV\text{-}I}$ and $C_{IV\text{-}II}$), where Salt #1, Salt #8, and Salt #9 exchanged positions, with Salt #5 consistently ranking among the most environmentally advantageous formulations.

Future research should focus on a detailed analysis of Molten Salt degradation mechanisms to establish strategies to minimize their environmental impact. This requires a thorough analysis and characterization of the elements and/or compounds that may adhere to or be released from the metallic components of CSP plants during corrosive and degradation processes (e.g., chromium, nickel, NO_x emissions), as these phenomena may influence the overall life-cycle environmental impacts. Similarly, additional research should examine how thermophysical properties, such as thermal conductivity, may impact the environmental performance of molten salts within actual CSP operating conditions. The objective is to rule out recycling scenarios that pose potential risks to human health and contribute to desertification (e.g., food additives, fertilizers). Furthermore, it would be interesting to carry out multidimensional feasibility studies to classify and prioritize the proposed recycling strategies based on environmental and techno-economic variables. The Analytic Hierarchy Process [96], or the Pareto front-based technique could be very useful tools to carry out this future research [97].

5. Conclusions

The method employed has demonstrated efficacy in characterizing, evaluating, and comparing the environmental impacts of various low-melting point Molten Salt formulations. This approach facilitates the identification of formulations exhibiting optimal environmental performance relative to heat transfer efficiency.

The results show that Salt #2 and Salt #5 are the most favorable in 10 of the 22 midpoint impact categories. Consequently, Salt #2 demonstrated greater favorability in the WCHH, WCTE, and WCAE midpoint categories, whereas Salt #5 was more favorable in the GWHH, GWTE, GWFE, SODP, OFHH, OFTE, and TA midpoint categories. Similarly, Salt #5 emerged as the most favorable Molten Salt within the three endpoint protection areas assessed (Human Health, Ecosystem Quality, and Resource Availability). Notably, Salt #5 was identified as the most favorable solution, exhibiting a favorability score up to 1.44 times higher than the average and up to 1.86 times that of traditional Solar Salt per kg of Molten Salt.

The presence of lithium nitrates also allows for increased energy efficiency, resulting in a direct reduction in the mass required to transfer the same amount of energy (1 MJ, functional unit). These results suggest that optimizing molten salts for CSP applications should prioritize formulations with high specific heat capacity and low mass per unit of heat transfer, as these parameters strongly influence both thermophysical and environmental performance. In this regard, Salt #5 requires only 1.22 kg of salt to achieve this functional unit, with an associated cost of 2.88 €/MJ. This improvement in efficiency is also reflected in its environmental performance, exhibiting values 1.82 times more favorable than the mean and up to 3.52 times more favorable than Solar Salt per Megajoule transferred. Furthermore, the sensitivity analysis confirmed the robustness of the proposed comparative framework, with Salt #5 consistently maintaining one of the most favorable environmental performances across the different scenarios and case studies evaluated.

Consistent with its outstanding environmental performance, Salt #5 is also identified as a preferred candidate for advanced thermal storage in CSP systems, due to its wide operating temperature range (469 °C) and its exceptional thermophysical properties, especially its high specific heat capacity of 3.23 J/gºC, which significantly exceeds the performance of Solar Salt, thus reinforcing its suitability for high-temperature applications.

This study, therefore, offers a general and detailed overview of the environmental impacts associated with the different formulations of low-melting point Molten Salt, which allows for comparison and improvement in the decision criteria of the managers responsible for CSP plants/facilities.

Acknowledgements

This investigation has been funded by the Ministry of Science and Innovation of Spain under grant agreement **ID: PCI2022-135041-2 /MCIN/AEI/10.13039/501100011033/European Union NextGenerationEU/PRTR. ADVIAMOS:** Advancing innovations in molten salts. We acknowledge its support.

Disclosure statement

No potential conflict of interest was reported by the authors.

Data availability statement

Data will be made available on request.

References

[1] D.A. Baharoon, H.A. Rahman, W.Z.W. Omar, S.O. Fadhl, Historical development of concentrating solar power technologies to generate clean electricity efficiently – A review, Renew. Sustain. Energy Rev. 41 (2015) 996–1027. https://doi.org/10.1016/j.rser.2014.09.008.

[2] X. Cai, Q. Miao, C. Huang, J. Xu, Y. Miao, Y. Liu, S. Liu, L. Yu, Dispatch optimization for off-grid hybrid CSP-PV combined heat and power system considering thermoelectric decoupling, Appl. Therm. Eng. 300 (2026) 131141. https://doi.org/10.1016/j.applthermaleng.2026.131141.

[3] M. Adio, R. Liberatore, G. Giannuzzi, E. Veca, D. Nicolini, M. Lanchi, M. Chieruzzi, ENEA research and innovation on Thermal Energy Storage for CSP plants, 2016.
[4] Z. Elmaazouzi, M. El Alami, H. Agalit, E.G. Bennouna, Performance evaluation of latent heat TES system-case study: Dimensions improvements of annular fins exchanger, Energy Reports 6 (2020) 294–301. https://doi.org/10.1016/j.egyr.2019.08.059.
[5] W. Al-Aloosi, Y. Alaiwi, H. Hamzah, Thermal performance analysis in a parabolic trough solar collector with a novel design of inserted fins, Case Stud. Therm. Eng. 49 (2023) 103378. https://doi.org/10.1016/j.csite.2023.103378.
[6] X. Liu, Y. Zhong, J. Li, H. Wang, M. Wang, A Review of High-Temperature Molten Salt for Third-Generation Concentrating Solar Power, Energy Sci. Eng. 13 (2025) 456–474. https://doi.org/10.1002/ese3.2029.
[7] H. Li, X. Liu, H. Ye, Z. Zhang, Y. Wang, Z. Yu, T. Zhou, Y. Wu, Z. Wang, H. Zhou, Experimental investigation of heat transfer mechanisms and dynamic energy conversion behavior in a flue gas-molten salt heat exchanger, Appl. Therm. Eng. 300 (2026) 131244. https://doi.org/10.1016/j.applthermaleng.2026.131244.
[8] G. Peiró, J. Gasia, L. Miró, C. Prieto, L.F. Cabeza, Influence of the heat transfer fluid in a CSP plant molten salts charging process, Renew. Energy 113 (2017) 148–158. https://doi.org/10.1016/j.renene.2017.05.083.
[9] E. Bellos, C. Tzivanidis, A. Papadopoulos, Optical and thermal analysis of a linear Fresnel reflector operating with thermal oil, molten salt and liquid sodium, Appl. Therm. Eng. 133 (2018) 70–80. https://doi.org/10.1016/j.applthermaleng.2018.01.038.
[10] E. Batuecas, C. Mayo, R. Díaz, F.J. Pérez, Life Cycle Assessment of heat transfer fluids in parabolic trough concentrating solar power technology, Sol. Energy Mater. Sol. Cells 171 (2017) 91–97. https://doi.org/10.1016/j.solmat.2017.06.032.
[11] L. Crema, F. Alberti, E. Wackelgard, B. Rivolta, S. Hesse, L. Luminari, D. Hislop, B. Restall, Novel System for Distributed Energy Generation from a Small Scale Concentrated Solar Power, Energy Procedia 57 (2014) 447–456. https://doi.org/10.1016/j.egypro.2014.10.198.
[12] A. Bonk, S. Sau, N. Uranga, M. Hernaiz, T. Bauer, Advanced heat transfer fluids for direct molten salt line-focusing CSP plants, Prog. Energy Combust. Sci. 67 (2018) 69–87. https://doi.org/10.1016/j.pecs.2018.02.002.
[13] T. Deng, C. Wu, W. Zhang, K. Luo, Thermo-economic performance assessment of a liquid CO2 energy storage system with different sensible heat storage materials, Energy 326 (2025) 136214. https://doi.org/10.1016/j.energy.2025.136214.
[14] Y. Li, S. Wang, Q. Zhu, Preparation and study of quaternary molten salts for thermal energy storage applications, Sol. Energy Mater. Sol. Cells 282 (2025) 113358. https://doi.org/10.1016/j.solmat.2024.113358.
[15] V. Russo, G. Petroni, F. Rovense, M. Giorgetti, G. Napoli, G. Giorgi, W. Gaggioli, Experimental Testing Results on Critical Components for Molten Salt-Based CSP Systems, Energies 18 (2025) 198. https://doi.org/10.3390/en18010198.
[16] J. Chaves, M.I. Lasanta, G. García-Martín, M.T. de Miguel, F.J. Pérez, Degradation mechanism of AISI 316L, 321H, and 347H alloys in ternary molten salt vs solar salt, Results Eng. 25 (2025) 104051.

https://doi.org/10.1016/j.rineng.2025.104051.
[17] C. Villada, A. Bonk, T. Bauer, F. Bolívar, High-temperature stability of nitrate/nitrite molten salt mixtures under different atmospheres, Appl. Energy 226 (2018) 107–115. https://doi.org/10.1016/j.apenergy.2018.05.101.
[18] Y.Y. Chen, C.Y. Zhao, Thermophysical properties of Ca(NO3)2-NaNO3-KNO3 mixtures for heat transfer and thermal storage, Sol. Energy 146 (2017) 172–179. https://doi.org/10.1016/j.solener.2017.02.033.
[19] J. Chaves, M.I. Lasanta, M.T. de Miguel, G. García-Martín, F.J. Pérez, Dynamic pilot plant test comparison between two ferritic-martensitic alloys in ternary eutectic molten salt, Results Eng. 25 (2025) 104343. https://doi.org/10.1016/j.rineng.2025.104343.
[20] A.G. Fernández, J. Gomez-Vidal, E. Oró, A. Kruizenga, A. Solé, L.F. Cabeza, Mainstreaming commercial CSP systems: A technology review, Renew. Energy 140 (2019) 152–176. https://doi.org/10.1016/j.renene.2019.03.049.
[21] C.C. Kwasi-Effah, O. Ighodaro, H.O. Egware, A.I. Obanor, Characterization and comparison of the thermophysical property of ternary and quaternary salt mixtures for solar thermal power plant applications, Results Eng. 16 (2022) 100721. https://doi.org/10.1016/j.rineng.2022.100721.
[22] T. Delise, A.C. Tizzoni, M. Ferrara, M. Telling, L. Turchetti, N. Corsaro, S. Sau, S. Licoccia, Phase Diagram Predictive Model for a Ternary Mixture of Calcium, Sodium, and Potassium Nitrate, ACS Sustain. Chem. Eng. 8 (2020) 111–120. https://doi.org/10.1021/acssuschemeng.9b04472.
[23] L.F. Cabeza, A. Gutierrez, C. Barreneche, S. Ushak, Á.G. Fernández, A. Inés Fernádez, M. Grágeda, Lithium in thermal energy storage: A state-of-the-art review, Renew. Sustain. Energy Rev. 42 (2015) 1106–1112. https://doi.org/10.1016/j.rser.2014.10.096.
[24] M. Henríquez, L. Guerreiro, Á.G. Fernández, E. Fuentealba, Lithium nitrate purity influence assessment in ternary molten salts as thermal energy storage material for CSP plants, Renew. Energy 149 (2020) 940–950. https://doi.org/10.1016/j.renene.2019.10.075.
[25] A. Boretti, Optimizing Concentrated Solar Power: High-Temperature Molten Salt Thermal Energy Storage for Enhanced Efficiency, Energy Storage 6 (2024). https://doi.org/10.1002/est2.70059.
[26] C. Zheng, K. Cheng, D. Han, High-Temperature Molten Salt Heat Exchanger Technology: Research Advances, Challenges, and Future Perspectives, Energies 18 (2025) 3195. https://doi.org/10.3390/en18123195.
[27] E. Gurgenc, H.İ. Yamaç, M. Özabacı, C.A. Canbay, T. Gurgenc, M. Gür, H.F. Öztop, E.S. Shahanaghi, Interfacial and thermophysical engineering for enhanced thermal performance of boron carbide-modified HITEC nanocomposites in high-temperature thermal energy storage applications, J. Mater. Res. Technol. 42 (2026) 1589–1612. https://doi.org/10.1016/j.jmrt.2026.03.168.
[28] E. Gurgenc, H.F. Öztop, H.İ. Yamaç, C.A. Canbay, Ş.M. Şenocak, M. Özabacı, T. Gurgenc, M. Gür, B4C-based nanoenhancement on the thermophysical and stability performance of solar salt: a novel approach for high-temperature TES applications, Case Stud. Therm. Eng. 75 (2025) 107257. https://doi.org/10.1016/j.csite.2025.107257.
[29] E. Gurgenc, H.F. Öztop, H.İ. Yamaç, C.A. Canbay, Ş.M. Şenocak, M. Ozabacı, M. Gür, Novel boride-enhanced solar salts: Thermophysical and structural properties for thermal energy storage, J. Energy Storage 143 (2026) 119207. https://doi.org/10.1016/j.est.2025.119207.

[30] E. Gurgenc, H.İ. Yamaç, M. Öztop, M. Özabacı, C.A. Canbay, T. Gurgenc, M. Gür, H.F. Öztop, Performance enhancement of Hitec molten salt through TiB2 and ZrB2 nanoadditives for High-Temperature TES and CSP applications, Sol. Energy Mater. Sol. Cells 301 (2026) 114298. https://doi.org/10.1016/j.solmat.2026.114298.

[31] I. Baklouti, M.A. Mujeebu, M.M. Noor, Next-generation renewable thermal systems: A roadmap for integration, intelligence, and decarbonization, Appl. Therm. Eng. 295 (2026) 130618. https://doi.org/10.1016/j.applthermaleng.2026.130618.

[32] A.R. Gamarra, S. Banacloche, Y. Lechon, P. del Río, Assessing the sustainability impacts of concentrated solar power deployment in Europe in the context of global value chains, Renew. Sustain. Energy Rev. 171 (2023) 113004. https://doi.org/10.1016/j.rser.2022.113004.

[33] I. Arias, J. Cardemil, E. Zarza, L. Valenzuela, R. Escobar, Latest developments, assessments and research trends for next generation of concentrated solar power plants using liquid heat transfer fluids, Renew. Sustain. Energy Rev. 168 (2022) 112844. https://doi.org/10.1016/j.rser.2022.112844.

[34] S. Kedar, H. Shinde, G.V. More, D. Watvisave, A. Bhosale, A critical review on solar applications of parabolic trough collector, J. Therm. Anal. Calorim. 150 (2025) 4907–4926. https://doi.org/10.1007/s10973-025-14094-y.

[35] M. Cellura, L.Q. Luu, F. Guarino, S. Longo, A review on life cycle assessment of concentrating solar energy technologies, Renew. Energy 249 (2025) 123203. https://doi.org/10.1016/j.renene.2025.123203.

[36] C.-C. Cormos, Solar-based calcium looping power plant with thermo-chemical energy storage capability: A techno-economic and environmental (LCA) analysis, Renew. Energy 251 (2025) 123431. https://doi.org/10.1016/j.renene.2025.123431.

[37] V. Piemonte, M. De Falco, P. Tarquini, A. Giaconia, Life Cycle Assessment of a high temperature molten salt concentrated solar power plant, Sol. Energy 85 (2011) 1101–1108. https://doi.org/10.1016/j.solener.2011.03.002.

[38] I.A.S. Ehtiwesh, M.C. Coelho, A.C.M. Sousa, Exergetic and environmental life cycle assessment analysis of concentrated solar power plants, Renew. Sustain. Energy Rev. 56 (2016) 145–155. https://doi.org/10.1016/j.rser.2015.11.066.

[39] N. Ko, M. Lorenz, R. Horn, H. Krieg, M. Baumann, Sustainability Assessment of Concentrated Solar Power (CSP) Tower Plants – Integrating LCA, LCC and LCWE in One Framework, Procedia CIRP 69 (2018) 395–400. https://doi.org/10.1016/j.procir.2017.11.049.

[40] R. Li, H. Zhang, H. Wang, Q. Tu, X. Wang, Integrated hybrid life cycle assessment and contribution analysis for CO2 emission and energy consumption of a concentrated solar power plant in China, Energy 174 (2019) 310–322. https://doi.org/10.1016/j.energy.2019.02.066.

[41] G. Gasa, A. Lopez-Roman, C. Prieto, L.F. Cabeza, Life Cycle Assessment (LCA) of a Concentrating Solar Power (CSP) Plant in Tower Configuration with and without Thermal Energy Storage (TES), Sustainability 13 (2021) 3672. https://doi.org/10.3390/su13073672.

[42] G. Gasa, C. Prieto, A. Lopez-Roman, L.F. Cabeza, Life cycle assessment (LCA) of a concentrating solar power (CSP) plant in tower configuration with different storage capacity in molten salts, J. Energy Storage 53 (2022) 105219. https://doi.org/10.1016/j.est.2022.105219.

[43] T. Xiao, C. Liu, X. Wang, S. Wang, X. Xu, Q. Li, X. Li, Life cycle assessment of

the solar thermal power plant integrated with air-cooled supercritical CO2 Brayton cycle, Renew. Energy 182 (2022) 119–133. https://doi.org/10.1016/j.renene.2021.10.001.

[44] X. Qi, X. Yao, P. Guo, Y. Han, L. Liu, Applying life cycle assessment to investigate the environmental impacts of a PV–CSP hybrid system, Renew. Energy 227 (2024) 120575. https://doi.org/10.1016/j.renene.2024.120575.

[45] X. Qi, X. Yao, P. Guo, Y. Chang, L. Liu, Y. Han, Applying LCA and cost–benefit analysis to evaluate the environmental impact and economic performance of hybrid PV-CSP plants, Environ. Dev. Sustain. (2025). https://doi.org/10.1007/s10668-025-06073-y.

[46] J.T. Adeoye, Y.M. Amha, V.H. Poghosyan, K. Torchyan, H.A. Arafat, Comparative LCA of Two Thermal Energy Storage Systems for Shams1 Concentrated Solar Power Plant: Molten Salt vs. Concrete, J. Clean Energy Technol. (2014) 274–281. https://doi.org/10.7763/JOCET.2014.V2.139.

[47] L. Miró, E. Oró, D. Boer, L.F. Cabeza, Embodied energy in thermal energy storage (TES) systems for high temperature applications, Appl. Energy 137 (2015) 793–799. https://doi.org/10.1016/j.apenergy.2014.06.062.

[48] Y. Lalau, X. Py, A. Meffre, R. Olives, Comparative LCA Between Current and Alternative Waste-Based TES for CSP, Waste and Biomass Valorization 7 (2016) 1509–1519. https://doi.org/10.1007/s12649-016-9549-6.

[49] S. Thaker, A.O. Oni, E. Gemechu, A. Kumar, Evaluating energy and greenhouse gas emission footprints of thermal energy storage systems for concentrated solar power applications, J. Energy Storage 26 (2019) 100992. https://doi.org/10.1016/j.est.2019.100992.

[50] D. Le Roux, R. Olivès, P. Neveu, Multi-objective optimisation of a thermocline thermal energy storage integrated in a concentrated solar power plant, Energy 300 (2024) 131548. https://doi.org/10.1016/j.energy.2024.131548.

[51] S.K. Suraparaju, M. Samykano, K. Kadirgama, R.K. Rajamony, Z. Said, A.K. Pandey, Integrating nanomaterials into phase change materials: Trends and future pathways for thermal energy storage, Appl. Therm. Eng. 298 (2026) 131108. https://doi.org/10.1016/j.applthermaleng.2026.131108.

[52] I. Ramón-Álvarez, E. Batuecas, S. Sánchez-Delgado, M. Torres-Carrasco, Mechanical performance after high-temperature exposure and Life Cycle Assessment (LCA) according to unit of stored energy of alternative mortars to Portland cement, Constr. Build. Mater. 365 (2023) 130082. https://doi.org/10.1016/j.conbuildmat.2022.130082.

[53] C.A.A. Vielma Leal, A. Calderón Díaz, A. Svobodova, Comparative life cycle assessment (LCA): Conventional TES system versus alternative steel slag-based TES system for CSP plants . Master in Renewable Energy and Energy Sustainability, (2023) 2022–2023.

[54] L. Betancor-Cazorla, C.A. Vielma, J. Mañosa, S. Dosta, J.M. Chimenos, C. Barreneche, Development of ternary blended cements (LC3) to be applied as thermal energy storage material in concentrated solar power plants, J. Energy Storage 133 (2025) 118023. https://doi.org/10.1016/j.est.2025.118023.

[55] V. Chinnasamy, G.K. Kalimuthu, Development of Advanced Heat Transfer Fluids for High-Temperature Solar Thermal Systems, in: 2025: pp. 251–273. https://doi.org/10.1007/978-981-96-5914-2_7.

[56] M. Botejara-Antúnez, J. González-Domínguez, F.J. Rebollo-Castillo, J. García-Sanz-Calcedo, Life cycle and environmental impact assessment of heat transfer fluids in parabolic trough CSP plants, Sustain. Energy Technol. Assessments 74

(2025) 104188. https://doi.org/10.1016/j.seta.2025.104188.
[57] International Organization for Standardization, Environmental Management - Life Cycle Assessment - Principles and Framework (ISO 14040:2006/Amd1:2021), (2021).
[58] International Organization for Standardization, Environmental Management - Life Cycle Assessment - Requirements and Guidelines (ISO 14044:2006/Amd1:2021), (2021).
[59] PRé Sustainability B.V., SimaPro 10.1, (2025).
[60] Ecoinvent Association, Ecoinvent 3.11, 2024.
[61] E. Crenna, M. Secchi, L. Benini, S. Sala, Global environmental impacts: data sources and methodological choices for calculating normalization factors for LCA, Int. J. Life Cycle Assess. 24 (2019) 1851–1877. https://doi.org/10.1007/s11367-019-01604-y.
[62] M.A.J. Huijbregts, Z.J.N. Steinmann, P.M.F. Elshout, G. Stam, F. Verones, M. Vieira, M. Zijp, A. Hollander, R. van Zelm, ReCiPe2016: a harmonised life cycle impact assessment method at midpoint and endpoint level, Int. J. Life Cycle Assess. 22 (2017) 138–147. https://doi.org/10.1007/s11367-016-1246-y.
[63] H. Martín, J. de la Hoz, G. Velasco, M. Castilla, J.L. García de Vicuña, Promotion of concentrating solar thermal power (CSP) in Spain: Performance analysis of the period 1998–2013, Renew. Sustain. Energy Rev. 50 (2015) 1052–1068. https://doi.org/10.1016/j.rser.2015.05.062.
[64] H. Benoit, L. Spreafico, D. Gauthier, G. Flamant, Review of heat transfer fluids in tube-receivers used in concentrating solar thermal systems: Properties and heat transfer coefficients, Renew. Sustain. Energy Rev. 55 (2016) 298–315. https://doi.org/10.1016/j.rser.2015.10.059.
[65] Y. Krishna, M. Faizal, R. Saidur, K.C. Ng, N. Aslfattahi, State-of-the-art heat transfer fluids for parabolic trough collector, Int. J. Heat Mass Transf. 152 (2020) 119541. https://doi.org/10.1016/j.ijheatmasstransfer.2020.119541.
[66] T. Wang, S. Viswanathan, D. Mantha, R.G. Reddy, Thermal conductivity of the ternary eutectic LiNO3–NaNO3–KNO3 salt mixture in the solid state using a simple inverse method, Sol. Energy Mater. Sol. Cells 102 (2012) 201–207. https://doi.org/https://doi.org/10.1016/j.solmat.2012.02.030.
[67] Y. Zhong, M. Wang, H. Wang, J. Yuan, Thermodynamic description of the quaternary Mg(NO3)2–KNO3–NaNO3–LiNO3 system and investigation on the novel Mg(NO3)2 based nitrate salts with low temperature, Sol. Energy Mater. Sol. Cells 230 (2021) 111148. https://doi.org/10.1016/j.solmat.2021.111148.
[68] A.G. Fernández, S. Ushak, H. Galleguillos, F.J. Pérez, Development of new molten salts with LiNO3 and Ca(NO3)2 for energy storage in CSP plants, Appl. Energy 119 (2014) 131–140. https://doi.org/10.1016/j.apenergy.2013.12.061.
[69] R.W. Bradshaw, D.E. Meeker, High-temperature stability of ternary nitrate molten salts for solar thermal energy systems, Sol. Energy Mater. 21 (1990) 51–60. https://doi.org/10.1016/0165-1633(90)90042-Y.
[70] Á.G. Fernández, S. Veliz, E. Fuentealba, H. Galleguillos, Thermal characterization of solar salts from north of Chile and variations of their properties over time at high temperature, J. Therm. Anal. Calorim. 128 (2017) 1241–1249. https://doi.org/10.1007/s10973-016-6037-y.
[71] T. Bauer, D. Laing, R. Tamme, Recent Progress in Alkali Nitrate/Nitrite Developments for Solar Thermal Power Applications, in: Molten Salts Chem. Technol., Wiley, 2014: pp. 543–553. https://doi.org/10.1002/9781118448847.ch7c.

[72] R.I. Olivares, W. Edwards, LiNO3–NaNO3–KNO3 salt for thermal energy storage: Thermal stability evaluation in different atmospheres, Thermochim. Acta 560 (2013) 34–42. https://doi.org/10.1016/j.tca.2013.02.029.
[73] D. Mantha, T. Wang, R.G. Reddy, Thermodynamic modeling of eutectic point in the LiNO3–NaNO3–KNO3–NaNO2 quaternary system, Sol. Energy Mater. Sol. Cells 118 (2013) 18–21. https://doi.org/10.1016/j.solmat.2013.06.023.
[74] F.J. Ruiz-Cabañas, C. Prieto, R. Osuna, V. Madina, A.I. Fernández, L.F. Cabeza, Corrosion testing device for in-situ corrosion characterization in operational molten salts storage tanks: A516 Gr70 carbon steel performance under molten salts exposure, Sol. Energy Mater. Sol. Cells 157 (2016) 383–392. https://doi.org/10.1016/j.solmat.2016.06.005.
[75] M.Z. Hauschild, R.K. Rosenbaum, S.I. Olsen, eds., Life Cycle Assessment, Springer International Publishing, Cham, 2018. https://doi.org/10.1007/978-3-319-56475-3.
[76] A.H. Alami, A.G. Olabi, A. Mdallal, A. Rezk, A. Radwan, S.M.A. Rahman, S.K. Shah, M.A. Abdelkareem, Concentrating solar power (CSP) technologies: Status and analysis, Int. J. Thermofluids 18 (2023) 100340. https://doi.org/10.1016/j.ijft.2023.100340.
[77] M.S. Praveen Kumar V, Analysis of Heat Transfer Fluids in Concentrated Solar Power (CSP) A Review Paper, Int. J. Eng. Res. Technol. 3 (2014) 239–240. www.ijert.org.
[78] A. Bonk, S. Sau, N. Uranga, M. Hernaiz, T. Bauer, Advanced heat transfer fluids for direct molten salt line-focusing CSP plants, Prog. Energy Combust. Sci. 67 (2018) 69–87. https://doi.org/10.1016/j.pecs.2018.02.002.
[79] H.M. Ali, T. Rehman, M. Arıcı, Z. Said, B. Duraković, H.I. Mohammed, R. Kumar, M.K. Rathod, O. Buyukdagli, M. Teggar, Advances in thermal energy storage: Fundamentals and applications, Prog. Energy Combust. Sci. 100 (2024) 101109. https://doi.org/10.1016/j.pecs.2023.101109.
[80] T. Bauer, C. Odenthal, A. Bonk, Molten Salt Storage for Power Generation, Chemie Ing. Tech. 93 (2021) 534–546. https://doi.org/10.1002/cite.202000137.
[81] A. Giaconia, G. Iaquaniello, A.A. Metwally, G. Caputo, I. Balog, Experimental demonstration and analysis of a CSP plant with molten salt heat transfer fluid in parabolic troughs, Sol. Energy 211 (2020) 622–632. https://doi.org/10.1016/j.solener.2020.09.091.
[82] Ministerio para la Transición Ecológica y el Reto Demográfico (Gobierno de España), Real Decreto 646/2020, de 7 de julio, por el que se regula la eliminación de residuos mediante depósito en vertedero, España, 2020.
[83] G.A. Rhys-Tyler, W. Legassick, M.C. Bell, The significance of vehicle emissions standards for levels of exhaust pollution from light vehicles in an urban area, Atmos. Environ. 45 (2011) 3286–3293. https://doi.org/10.1016/j.atmosenv.2011.03.035.
[84] L. van Oers, J.B. Guinée, R. Heijungs, R. Schulze, R.A.F. Alvarenga, J. Dewulf, J. Drielsma, D. Sanjuan-Delmás, T.C. Kampmann, G. Bark, A.G. Uriarte, P. Menger, M. Lindblom, L. Alcon, M.S. Ramos, J.M.E. Torres, Top-down characterization of resource use in LCA: from problem definition of resource use to operational characterization factors for dissipation of elements to the environment, Int. J. Life Cycle Assess. 25 (2020) 2255–2273. https://doi.org/10.1007/s11367-020-01819-4.
[85] A. Roesch, S. Sala, N. Jungbluth, Normalization and weighting: the open challenge in LCA, Int. J. Life Cycle Assess. 25 (2020) 1859–1865.

https://doi.org/10.1007/s11367-020-01790-0.
[86] E. Gürgenç, H.F. Öztop, Ş.M. Şenocak, C. Aktemur, T. Gürgenç, Y. Varol, H.İ. Yamaç, M. Gür, Hafnium carbide as a novel nanofiller for RT64HC phase change materials: Enhancing thermal conductivity, heat capacity, and cycling stability, Therm. Sci. Eng. Prog. 69 (2026) 104257. https://doi.org/10.1016/j.tsep.2025.104257.
[87] E. Bakır Gür, E. Işık, A. Uçar, Numerical analysis of PCM integrated in solar dryers for thermal efficiency, Ain Shams Eng. J. 17 (2026) 103847. https://doi.org/10.1016/j.asej.2025.103847.
[88] Y.Y. Chen, C.Y. Zhao, Thermophysical properties of Ca(NO3)2-NaNO3-KNO3 mixtures for heat transfer and thermal storage, Sol. Energy 146 (2017) 172–179. https://doi.org/10.1016/j.solener.2017.02.033.
[89] C.C. Kwasi-Effah, O. Unuareokpa, H.O. Egware, O. Ighodaro, A.I. Obanor, U. Onoche, J. Achebo, Enhancing thermal conductivity of novel ternary nitrate salt mixtures for thermal energy storage (TES) fluid, Prog. Eng. Sci. 1 (2024) 100020. https://doi.org/10.1016/j.pes.2024.100020.
[90] Y. Yu, Y. Wang, Y. Ao, H. Tian, X. Wu, Thermal properties enhancement of recycled lithium chloride molten salt doped with SiC used for thermal energy storage: A molecular dynamics study, Int. Commun. Heat Mass Transf. 157 (2024) 107734. https://doi.org/10.1016/j.icheatmasstransfer.2024.107734.
[91] O. Verbitsky, S. Pushkar, Eco-Indicator 99, ReCiPe and ANOVA for evaluating building technologies under LCA uncertainties, Environ. Eng. Manag. J. 17 (2018) 2549–2559. https://doi.org/10.30638/eemj.2018.253.
[92] L. Van Oers, CML-IA database, characterisation and normalisation factors for midpoint impact category indicators, Version 4 (2015) 5.
[93] I. Sazdovski, A. Bala, P. Fullana-i-Palmer, Linking LCA literature with circular economy value creation: A review on beverage packaging, Sci. Total Environ. 771 (2021) 145322. https://doi.org/10.1016/j.scitotenv.2021.145322.
[94] M. Botejara-Antúnez, J. González-Domínguez, J. García-Sanz-Calcedo, Comparative analysis of flat roof systems using life cycle assessment methodology: Application to healthcare buildings, Case Stud. Constr. Mater. 17 (2022) e01212. https://doi.org/10.1016/j.cscm.2022.e01212.
[95] E. Kisel, A. Hamburg, M. Härm, A. Leppiman, M. Ots, Concept for Energy Security Matrix, Energy Policy 95 (2016) 1–9. https://doi.org/10.1016/j.enpol.2016.04.034.
[96] M. Botejara-Antúnez, J. González-Domínguez, G. Sánchez-Barroso, J. García-Sanz-Calcedo, Optimal selection of false ceiling systems in healthcare buildings: a multidimensional hierarchical analysis for sustainability, Archit. Eng. Des. Manag. 20 (2024) 1815–1831. https://doi.org/10.1080/17452007.2023.2291586.
[97] S. Ghosh, M.C. Mandal, A. Ray, Investigating the Key Performance Parameters of Green Supply Chain Management for Sustainability in Tea Processing Firms Using Pareto Analysis, J. Inst. Eng. Ser. C 104 (2023) 113–122. https://doi.org/10.1007/s40032-022-00888-8.

Declaration of interests

☒ The authors declare that they have no known competing financial interests or personal relationships that could have appeared to influence the work reported in this paper.

☐ The authors declare the following financial interests/personal relationships which may be considered as potential competing interests:

Highlights

- LCA provides clear insight into environmental impacts of low-melting point Molten Salts.
- Cradle-to-grave approach ensures robust sustainability assessment of Molten Salts.
- $LiNO_3$-based Molten Salts combine superior heat capacity and operational performance.
- Salt #5 offers the lowest environmental impact with intermediate cost.
- Solar Salt exhibits the highest environmental burden among assessed Molten Salts.